Published in final edited form as:

Cancer Res. 2021 April 01; 81(7): 1667–1680. doi:10.1158/0008-5472.CAN-20-0177.

Germline and Somatic Genetic Variants in the p53 Pathway Interact to Affect Cancer Risk, Progression, and Drug Response

Ping Zhang[1], **Isaac Kitchen-Smith**[1], **Lingyun Xiong**[1], **Giovanni Stracquadanio**[1], **Katherine Brown**[2], **Philipp H. Richter**[1], **Marsha D. Wallace**[1], **Elisabeth Bond**[1], **Natasha Sahgal**[1], **Samantha Moore**[1], **Svanhild Nornes**[1], **Sarah De Val**[1], **Mirvat Surakhy**[1], **David Sims**[2], **Xuting Wang**[3], **Douglas A. Bell**[3], **Jorge Zeron-Medina**[1,5], **Yanyan Jiang**[4], **Anderson J. Ryan**[4], **Joanna L. Selfe**[5], **Janet Shipley**[5], **Siddhartha Kar**[6], **Paul D. Pharoah**[6], **Chey Loveday**[7], **Rick Jansen**[8], **Lukasz F. Grochola**[9], **Claire Palles**[10], **Andrew Protheroe**[12], **Val Millar**[13], **Daniel V. Ebner**[13], **Meghana Pagadala**[14], **Sarah P. Blagden**[11], **Timothy S. Maughan**[11], **Enric Domingo**[11], **Ian Tomlinson**[10], **Clare Turnbull**[7], **Hannah Carter**[14], **Gareth L. Bond**[1]

[1]Ludwig Institute for Cancer Research, University of Oxford, Nuffield Department of Clinical Medicine, Old Road Campus Research Building, Oxford, United Kingdom.

[2]Weatherall Institute of Molecular Medicine, University of Oxford, John Radcliffe Hospital, Oxford, United Kingdom.

[3]Environmental Epigenomics and Disease Group, Immunity, Inflammation, and Disease Laboratory, National Institute of Environmental Health Sciences-National Institutes of Health, Research Triangle Park, North Carolina.

[4]CRUK & MRC Oxford Institute for Radiation Oncology, University of Oxford, Department of Oncology, Old Road Campus Research Building, Oxford, United Kingdom.

Corresponding Authors: Gareth L. Bond, Institute for Cancer and Genomic Sciences, University of Birmingham, Birmingham, B15 2TT, United Kingdom. G.Bond.1@bham.ac.uk; and Hannah Carter, UCSD, 9500 Gilman Drive, La Jolla, CA 92093. hkcarter@health.ucsd.edu.

Current address for P. Zhang and M.D. Wallace, Wellcome Centre for Human Genetics, University of Oxford, Oxford, United Kingdom; current address for G. Stracquadanio, Institute of Quantitative Biology, Biochemistry, and Biotechnology, SynthSys, School of Biological Sciences, University of Edinburgh, Edinburgh, United Kingdom; current address for K. Brown, Division of Virology, Department of Pathology, University of Cambridge, Cambridge, United Kingdom; Current address for J. Zeron-Medina, Translational Medicine, Research and Early Development, Oncology R&D, AstraZeneca, Waltham, Massachusetts; current address S. Kar, MRC Integrative Epidemiology Unit, Population Health Sciences, Bristol Medical School, University of Bristol, United Kingdom; current address for S. Nornes and S. De Val, Department of Physiology, Anatomy and Genetics, University of Oxford, United Kingdom; current address for Gareth L. Bond, Institute of Cancer and Genomic Sciences, University of Birmingham, Birmingham, United Kingdom.

Authors' Contributions

P. Zhang: Data curation, formal analysis, visualization, methodology, writing–original draft, writing–review and editing. **I. Kitchen-Smith:** Data curation, formal analysis, validation, writing–review and editing. **L. Xiong:** Data curation, formal analysis, validation, writing–review and editing. **G. Stracquadanio:** Data curation, methodology, writing–review and editing. **K. Brown:** Data curation. **P.H. Richter:** Data curation, validation. **M.D. Wallace:** Methodology. **E. Bond:** Data curation. **N. Sahgal:** Methodology. **S. Moore:** Validation. **S. Nornes:** Data curation. **S. De Val:** Methodology. **M. Surakhy:** Validation. **D. Sims:** Methodology. **X. Wang:** Resources, methodology. **D.A. Bell:** Resources, methodology, writing–review and editing. **J. Zeron-Medina:** Resources. **Y. Jiang:** Data curation, formal analysis. **A.J. Ryan:** Data curation, formal analysis. **J.L. Selfe:** Methodology. **J. Shipley:** Methodology. **S. Kar:** Resources, methodology. **P.D. Pharoah:** Resources, methodology. **C. Loveday:** Resources. **R. Jansen:** Resources. **L.F. Grochola:** Methodology. **C. Palles:** Methodology. **A. Protheroe:** Methodology. **V. Millar:** Data curation, formal analysis. **D.V. Ebner:** Data curation, formal analysis. **M. Pagadala:** Data curation, formal analysis. **S.P. Blagden:** Methodology, writing–review and editing. **T.S. Maughan:** Resources, methodology. **E. Domingo:** Resources, methodology. **I. Tomlinson:** Resources, methodology, writing–review and editing. **C. Turnbull:** Resources, data curation, methodology, writing–review and editing. **H. Carter:** Conceptualization, formal analysis, investigation, methodology, writing–original draft, writing–review and editing. **G.L. Bond:** Conceptualization, formal analysis, investigation, methodology, writing–original draft, project administration, writing–review and editing.

Supplementary data for this article are available at Cancer Research Online (http://cancerres.aacrjournals.org/).

[5]Sarcoma Molecular Pathology Team, Divisions of Molecular Pathology and Cancer Therapeutics, The Institute of Cancer Research, Sutton, Surrey, United Kingdom.

[6]Department of Public Health and Primary Care, University of Cambridge, Cambridge, United Kingdom.

[7]Division of Genetics and Epidemiology, The Institute of Cancer Research, London, United Kingdom.

[8]Amsterdam UMC, Vrije Universiteit Amsterdam, Department of Psychiatry, Amsterdam Neuroscience, the Netherlands.

[9]Department of Surgery, Cantonal Hospital Winterthur, Switzerland.

[10]Institute of Cancer and Genomic Sciences, University of Birmingham, Birmingham, United Kingdom.

[11]Department of Oncology, University of Oxford, Oxford, United Kingdom.

[12]Oxford Cancer and Haematology Centre, Oxford University Hospitals NHS Foundation Trust, Oxford, United Kingdom.

[13]Target Discovery Institute, University of Oxford, Nuffield Department of Medicine, Oxford, United Kingdom.

[14]Department of Medicine, University of California, San Diego, La Jolla, California.

Abstract

Insights into oncogenesis derived from cancer susceptibility loci (SNP) hold the potential to facilitate better cancer management and treatment through precision oncology. However, therapeutic insights have thus far been limited by our current lack of under standing regarding both interactions of these loci with somatic cancer driver mutations and their influence on tumorigenesis. For example, although both germline and somatic genetic variation to the p53 tumor suppressor pathway are known to promote tumorigenesis, little is known about the extent to which such variants cooperate to alter pathway activity. Here we hypothesize that cancer risk-associated germline variants interact with somatic *TP53* mutational status to modify cancer risk, progression, and response to therapy. Focusing on a cancer risk SNP (rs78378222) with a well-documented ability to directly influence p53 activity as well as integration of germline datasets relating to cancer susceptibility with tumor data capturing somatically-acquired genetic variation provided supportive evidence for this hypothesis. Integration of germline and somatic genetic data enabled identification of a novel entry point for therapeutic manipulation of p53 activities. A cluster of cancer risk SNPs resulted in increased expression of prosurvival p53 target gene *KITLG* and attenuation of p53-mediated responses to genotoxic therapies, which were reversed by pharmacologic inhibition of the prosurvival c-KIT signal. Together, our results offer evidence of how cancer susceptibility SNPs can interact with cancer driver genes to affect cancer progression and identify novel combinatorial therapies.

Introduction

Efforts to characterize the somatic alterations that drive oncogenesis have led to the development of targeted therapies, facilitating precision approaches that condition treatment on knowledge of the tumor genome, and improving outcomes for many patients with cancer (1, 2). However, such targeted therapies are associated with variable responses, eventual high failure rates and the development of drug resistance. Somatic genetic heterogeneity among tumors is a major factor contributing to differences in disease progression and therapeutic response (1). Inter-individual differences may arise not only from different somatic alterations, but also from differences in the underlying genetic background. The maps of common germline genetic variants that associate with disease susceptibility allow us to generate and test biological hypotheses, characterize regulatory mechanisms by which variants contribute to disease, with the aim of integrating the results into the clinic. However, there are challenges in harnessing susceptibility loci for target identification for cancer, including limitations in (i) exposition of causative variants within susceptibility loci, (ii) understanding of interactions of susceptibility variants with somatic driver mutations, and (iii) mechanistic insights into their influence on cellular behaviors during and after the evolution of somatic cancer genomes (3–5).

A key cancer signaling pathway known to harbor multiple germline and somatic variants associated with cancer susceptibility is the p53 tumor suppressor pathway (6). It is a stress response pathway that maintains genomic integrity and is among the most commonly perturbed pathways in cancer, with somatic driver mutations found in the *TP53* gene in more than 50% of cancer genomes (7). Loss of the pathway and/or the gain of procancer mutations can lead to cellular transformation and tumorigenesis (8). Once cancer has developed, the p53 pathway is important in mediating cancer progression and the response to therapy, as its anticancer activities can be activated by many genotoxic anticancer drugs (9). These drugs are more effective in killing cancers with wild-type p53 relative to mutant p53 (10, 11). Although both germline and somatic alterations to the p53 pathway are known to promote tumorigenesis, the extent to which such variants cooperate to alter pathway activity and the effects on response to therapy remain poorly understood.

Most studies have separately examined the consequences of somatic and germline variation affecting p53 activity to understand their roles in disease risk, progression, or response to therapy. Here we hypothesize that cancer-associated germline variants (SNP) interact with *TP53* somatic driver mutations to modify cancer risk, progression, and potential to respond to therapy. With a focus on a cancer-associated SNP that directly influences p53 activity, we provide supportive evidence for this hypothesis, and go on to demonstrate how such germline–somatic interactions inform discovery of candidate drug targets.

Materials and Methods

Assigning *TP53* mutational status to breast cancer, ovarian cancer, and The Cancer Genome Atlas tumors

We curated *TP53* pathogenic missense mutations by integrating up-to-date functional evidence from both literature and databases as detailed in Supplementary Information.

In total, we were able to find 218 of 323 *TP53* pathogenic mutations are oncogenic (Supplementary Table S1). All *TP53* missense mutations in breast cancer, ovarian cancer, and The Cancer Genome Atlas (TCGA) primary tumors were extracted and matched with the curated lists of pathogenic and oncogenic *TP53* missense mutations.

Analysis for subtype heterogeneity SNPs with breast and ovarian cancer association studies

Estimates of effect sizes [log(OR)s] for subtype-specific case–control studies and their corresponding standard errors were utilized for meta- and heterogeneity-analyses using METAL (2011–03–25 release; ref. 12), under an inverse variance fixed-effect model. (See Supplementary Information for details.)

Cancer GWAS SNPs

We selected the GWAS significant lead SNPs (*P* value <5e–08) in Europeans, and retrieved the associated proxy SNPs using the 1,000 Genomes phase III data through the web server rAggr. (See Supplementary Information for details.)

Enrichment analysis

The hypergeometric distribution enrichment analysis was performed as described in ref. 6. Significance was determined using PHYPER function as implemented in R and multiple hypotheses testing by Benjamini–Hochberg correction.

Genotype imputation and population stratification

Genotype data were obtained and filtered as described in ref. 3. The genotype data of 7,021 patients with TCGA were clustered tightly with Europeans. (See Supplementary Information for details.)

TCGA survival analysis

The omics datasets (gene mutation, copy number, and mRNA expression) of the TCGA cohort were downloaded from the cBioPortal (https://www.cbioportal.org/). We considered those mutations with putative oncogenic properties (marked as “Oncogenic,” “Likely Oncogenic,” or “Predicted Oncogenic” in OncoKB) as oncogenic mutations. TCGA clinical data were downloaded from the recently updated Pan-Cancer Clinical Data Resource (TCGA-CDR; ref. 13). TCGA clinical radiation data were retrieved using R package TCGAbiolinks (V2.16.1). The patients with “Radiographic Progressive Disease” were defined as radiation nonresponders. Patients with “complete response” or “partial response” were defined as responders. A Cox proportional hazards regression model was used to calculate the HR, the 95% confidence interval (CI), and *P* values for the two-group comparisons. The log-rank test was used to compare the differences of Kaplan–Meier survival curves. The clinical, gene expression, and mutation data for the DFCI-SKCM cohort was downloaded from cBioPortal. The optimal cut-off of the gene expression for the survival analysis was determined using the survcutpoint function of the survminer R package, and used to stratify the patients into high- and low-risk groups.

GDSC drug sensitivity analysis

TP53 mutation, copy number, RNA-seq gene expression data, and drug IC_{50} values for the cancer cell lines were downloaded from Genomics of Drug Sensitivity in Cancer (GDSC; release-8.1). The classified cell lines based on *TP53* mutational status were further grouped on the basis of the gene transcript levels: low (≤1st quartile), intermediate (>1st quartile and <3rd quartile), and high (≥3rd quartile). The effects of the mutation status or transcript levels on drug sensitivity were then determined with a linear model approach. (See details in Supplementary Information.)

Cell culture and their treatments

Testicular cancer cell lines TERA1, TERA2, 2102EP, Susa-CR, GH, were cultured in RPMI medium containing 10% FBS and 1% penicillin/streptomycin according to standard conditions. Susa cells were cultured in RPMI medium containing 20% FBS and 1% penicillin/streptomycin. GCT27 and GCT27-CR were cultured in DMEM supplemented with 10% FBS and 1% penicillin/streptomycin. Hap1 cells were obtained from Horizon Discovery Ltd., and cultured in IMDM (Sigma-Aldrich Co. Ltd.) supplemented with 10% FBS and 1% penicillin/streptomycin. FuGENE 6 Transfection Reagent (Promega) was used for DNA transfection. For transfection of siRNA, Lipofectamine RNAiMAX Transfection Reagent (Thermo Fisher Scientific) was used. The cell lines were tested for mycoplasma contamination every 3 to 4 weeks using MycoAlert Mycoplasma Detection Kit (Lonza), and used for experiments at less than 20 passages. Cell line authentication was performed by short tandem repeat (STR) analysis (Eurofins Genomics).

CRISPR/Cas9-mediated genome editing

The Cas9 expression vector was obtained from Addgene (#62988). sgRNAs were designed and constructed as described previously (14). The oligo sequences for the sgRNA synthesis are listed in Supplementary Table S2. (See Supplementary Information for details.)

RNA isolation, qRT-PCR, and RNA-seq analysis

RNA isolation, qRT-PCR, and RNA-seq analysis were performed as detailed in Supplementary Information.

Drug screening

Cells were seeded in 384-well plates (flat bottom, black with clear bottom, Greiner) at density of about 2,000 cells per well in 81 mL with cell dispenser (Perkin-Elmer) and liquid handling robotics (JANUS, Perkin-Elmer) and incubated overnight. Next, library compounds (Supplementary Table S3) were added to a final concentration of 10 μmol/L, 1 μmol/L, 100 nmol/L, or 10 nmol/L. Dasatinib (1 μmol/L) was added as positive control and DMSO (Vehicle, 0.1%) was added as negative control. After 72 hours, cell were fixed with 4% paraformaldehyde for 10 minutes, permeabilized with 0.5% Triton X-100 for 5 minutes, and then stained with 1:1,000 dilution of 5 mg/mL DAPI for 5 minutes. Next, the plates were imaged using a high-content analysis system (Operetta, Perkin-Elmer). The image data were analyzed by an image data storage and analysis system (Columbus, Perkin-Elmer). The cells with nuclear area >150 and nuclear intensity <700 were counted, and cell number was used

as the viability readout. The screen was performed in duplicate. The Pearson correlation coefficient, a measurement for inter-assay variability, averaged 0.98 and an average *Z*-factor, a measure employed in high throughput screens to measure effect size, of 0.69for all plates was recorded, leading to high confidence in the primary screen positive hits (Supplementary Table S4).

SDS-PAGE and Western blotting

SDS-PAGE and Western blotting was performed as described in ref. 15. The antibodies against p53 (sc-126), c-KIT (sc-17806), PARP1 (sc-7150), and β-Actin (sc-47778) were from Santa Cruz Biotechnology. The antibodies against acetylated p53 (Lys382, #2525), cleaved caspase-3 (Asp175, #9661) were from Cell Signaling. HRP-coupled secondary antibodies were from Dako.

IC_{50} and combination index CI analyses

To determine an IC_{50}, eight multiply diluted concentrations were used including a PBS control for 48-hour treatments and then cell viability was assessed by a MTT assay (see details in Supplementary Information). The IC_{50} was calculated using the Graphpad Prism software. A constant ratio matrix approach was used to determine the combination index CI values (16). Single drug data and combination data was entered into Compusyn software (http://www.combosyn.com) to compute CI_{50} and dose-reduction index (DRI). CI_{50} is [CX/IC_{50}(X)] + [CY/IC_{50}(Y)], where [CX/IC_{50}(X)] is the ratio of the drug X's concentration (CX) in a 50% effective drug mixture to its 50% inhibitory concentration [IC_{50}(X)] when applied alone. The CI_{50} values quantitatively depict synergistic (CI < 1), additive (CI = 1), and antagonistic effects (CI > 1).

In vivo study

All animal procedures were carried out under a UK Home Office project license (PPL30/3395). Before submitting to the Home Office, the project license was approved by the Oxford University Animal Welfare and Ethical Review Board. Mice were housed at Oxford University Biomedical Services, UK. Six- to eight-week-old female BALB/c nude mice (Charles River) were injected subcutaneously. (See Supplementary Information for details.)

Results

p53 regulatory cancer risk SNP rs78378222 associates with subtype heterogeneity

To represent germline effects, we focused on the cancer risk-associated SNP with the most direct and most understood influence on p53 activity. This SNP, rs78378222, resides in the 3'-UTR in the canonical *TP53* polyadenylation signal [p53 poly(A) SNP]. The minor C-allele is known to associate with lower *TP53* mRNA levels in different normal tissue types, such as in blood, skin, adipose, esophagus-mucosa, and fibroblasts (17, 18), and associate strongly with differential risk of many cancer types (19–23).

We explored whether the p53 poly(A) SNP can differentially influence mutantand wild-type *TP53* (*wtTP53*) cancer risk by studying cancers with subtypes that differ substantially in

TP53 mutation frequencies and for which susceptibility GWAS data are available. Eighteen percent of estrogen receptor positive breast cancers (ER+BC) mutate *TP53*, in contrast to 76% of estrogen receptor negative breast cancers (ER-BC; ref. 24). Similarly, less than 10% of low-grade serous ovarian cancers (LGSOC) mutate *TP53*, in contrast to 96% of high-grade serous ovarian cancers (HGSOC; ref. 25). Over 85% of *TP53* pathogenic missense mutations in breast and ovarian cancers are oncogenic (either dominant negative or gain of function; Fig. 1A; see Materials and Methods). We analyzed data from 90,969 patients with breast cancer of European ancestry (69,501 ER+BC; 21,468 ER−BC; ref. 26) and 105,974 controls, and 14,049 patients with ovarian cancer of European ancestry (1,012 LGSOC; 13,037 HGSOC) and 40,941 controls (27).

It is known that key regulatory pathway genes and stress signals, which can regulate *wtTP53* levels and tumor suppressive activities, can also regulate mutant p53, including its oncogenic activities (28, 29). Thus, if the poly(A) SNP can inf1uence both mutant and *wtTP53* expression, the minor C-allele (less *TP53* expression) would be expected to have opposite associations with disease subtype (Fig. 1B). That is, the minor C-allele would associate with increased cancer risk (OR > 1) in the subtypes with low *TP53* mutation frequencies (ER BC and LGSOC), and decreased cancer risk (OR < 1) in the subtypes with high *TP53* mutation frequencies (ER-BC and HGSOC). Indeed, this is the case, whereby we found an increase in the frequency of the minor C-allele in patients with ER+BC and LGSOC compared with healthy controls (OR = 1.12; P = 1.0e-03 and OR = 1.59; P = 0.016, respectively; Fig. 1C), but a decreased frequency in ER-BC and HGSOC patients compared with controls (OR = 0.80; P = 2.3e–04 and OR = 0.75; P = 3.7e–04, respectively). Taken together, the distribution of minor C-allele shows significant heterogeneity among the four cancer subtypes (P_{het} 2.59e–09).

The above analysis supports a persistent effect for the p53 cancer risk SNP on tumors through a possible inf1uence on whether a tumor contains a somatically mutated *TP53* locus. To seek further and more direct support of this possibility, we performed similar analyses of the p53 poly(A) SNP in a cohort of 7,021 patients of European origin diagnosed with 31 different cancers and for whom the *TP53* mutational status of their cancers could be determined (The Cancer Genome Atlas, TCGA). We partitioned the patients into two groups based on the presence or absence of the *TP53* somatic alteration (mutation and CNV loss vs. WT and no CNV loss; Fig. 1D). Interestingly, the p53 poly(A) SNP associated with allelic differences in minor allele frequencies (MAF) between the groups of patients with either *wtTP53* or mutant tumors (Fig. 1E). This is in line with the associations found with *TP53* mutational status of breast and ovarian cancer subtypes, whereby the C-allele is more frequent in *wtTP53* tumors.

A p53 regulatory cancer risk SNP can affect wild-type and mutant *TP53* in tumors, and associates with clinical outcomes

As mentioned above, the minor C-allele of the p53 poly(A) SNP has been previously found to associate with lower p53 mRNA levels in many different normal tissues and cells (18). To investigate the activity of this SNP in tumors, we analyzed expression data from 3,248 tumors from the TCGA cohort, for which both germline and somatic genetic data

are available and no somatic copy number variation of *TP53* could be detected. Similar to results obtained in the normal tissues, we observed a significant association of the minor C-allele with lower *TP53* expression levels in the tumors, estimated 1.5-fold per allele ($P = 1.7–04$; $\beta = -0.37$; Fig. 2A). To test if the C-allele associates with lower levels of both wild-type and mutant *TP53*, we divided the tumors into three groups based on their respective somatic *TP53* mutational status (Supplementary Fig. S1A; Supplementary Table S5). We found 2,521 tumors with *wtTP53*, 448 with missense mutations, and, of those, 389 with oncogenic missense mutations. In all three groups, the C-allele significantly associates with lower *TP53* expression levels (Supplementary Fig. S1B).

Next, we utilized Hap1 cells that contain a dominant-negative *TP53* missense mutation (p.S215G), which results in a mutated DNA-binding domain (30). We generated clones with either the A-allele or the C-allele (Fig. 2B), and found significantly lower *TP53* mRNA levels in cells with the C-allele relative to the A-allele (~2-fold, Fig. 2C). We also found the C-allele containing cells express less p53 protein (Supplementary Fig. S1C). The impairment of 3'-end processing and subsequent transcription termination by the minor allele of the p53 poly(A) SNP have been proposed as a mechanism for the genotype-dependent regulatory effects on *TP53* expression (17). Indeed, we observed significant enrichments of uncleaved *TP53* mRNA in cells carrying the C-allele compared with the A-allele by qRT-PCR and 3' RNA-sequencing (Supplementary Figs. S1D and S1E). Together, our data demonstrate that this cancer risk-associated SNP can inf1uence the expression of both wild-type and mutant *TP53* in cancer cells and tumors.

To explore whether the p53 poly(A) SNP also associates with allelic differences in clinical outcomes, we stratified the TCGA cohort into two groups based on *TP53* somatic alterations and the p53 poly(A) SNP genotypes. We found that in patients with *wtTP53* tumors, those with the minor C-alleles have a significantly shorter progression-free interval (PFI) and worse OS compared with those without the minor alleles (Fig. 2D), but not in patients without stratification. An inverted, but not significant trend, among the patients with somatic *TP53* mutations is noted. Similarly, significant, *TP53* mutational status-dependent, associations between the p53 poly(A) SNP and PFI can be found when we restrict our analyses to breast cancer patients only (Fig. 2E).

It is well documented that p53 somatic mutations antagonize cellular sensitivity to radiotherapy (31), an important component of current cancer treatments. Indeed, we see not only *TP53* mutations, but also the p53 poly(A) SNP play roles in the radiation response phenotype in the TCGA cohort. Specifically, we focused on the 7021 patients for whom the SNP genotypes were available. Of these, 848 patients could be assigned with radiation response phenotypes (603 responders; 134 nonresponders; see Materials and Methods). We determined that the radiation nonresponders were significantly enriched in patients with *TP53* somatic mutations (OR = 1.6; $P = 0.021$; Fig. 2F). The enrichment was further enhanced when we analyzed those patients with both *TP53* mutations and copy number loss (OR = 2.2; $P = 0.0026$). Importantly, we also found that in patients with *wtTP53* tumors, but not with *TP53* mutant tumors, radiation nonresponders were greatly enriched in the C-allele of the p53 poly(A) SNP (less *TP53* expression; OR = 5.6; $P = 0.011$ for risk allele; Fig. 2F).

Somatic copy number loss of *TP53* can mimic effects of the p53 poly(A) SNP

Together, the results we have presented thus-far suggest that the relative two-fold reduction of *wtTP53* levels in tumors from patients with the minor allele of the p53 regulatory SNP can lead to worse clinical outcomes and treatment response. If true, we reasoned that we should be able to find similar associations in patients whose tumors lose a single copy of *TP53*. In the TGCA database, 1,839 (26.6%) patients with *wtTP53* tumors, and 2,236 (59.3%) patients with mutant *TP53* tumors show significant signs of loss at the *TP53* locus (estimated one copy on average, GISTIC score 1). These tumors associate with 1.3- and 1.1-fold lower *TP53* RNA expression respectively compared with the tumors without loss (Fig. 2G). In support of small reductions of *TP53* expression affecting patient outcome, we found that *wtTP53*-loss associates with shorter PFI and worse OS compared with no *wtTP53*-losses (Fig. 2H), but are not found in patients with mutant *TP53*. These associations are independent of tumor type (adjusted $P < 0.05$; Fig. 2H). We also found in patients with *wtTP53* tumors that radiotherapy nonresponders are significantly enriched in cancers with *TP53* copy number loss (OR = 1.6; $P = 0.027$; Fig. 2I).

We next sought to test whether the modest changes in *TP53* expression (<2 fold) could predict chemosensitivities. We used the drug sensitivity dataset with both somatic genetic and gene expression data (GDSC; 304 drugs across 987 cell lines). Similar to what we observed in TCGA tumors, *TP53* copy number loss in cancer cell lines associates with a modest reduction in *TP53* expression (Fig. 3A). Strikingly, and as predicted, *wtTP53* loss, but not mutant *TP53*-loss, significantly associates with reduced sensitivities to 31% of the drugs tested (Fig. 3B; Supplementary Table S6). Specifically, 93 out of the 304 drugs demonstrated reduced sensitivity in *wtTP53* cell lines with *TP53*-loss compared with those without a loss (adjusted $P < 0.05$; Fig. 3B). These drugs included many known p53 activating agents including an MDM2 inhibitor (Nutlin3), as well as standard chemotherapeutics such as cisplatin, doxorubicin, and etoposide. Together, our observations clearly indicate that patients whose tumors have modest decreases in *wtTP53* expression, mediated either through the regulatory SNP or somatic *TP53* copy number loss, associate with poorer DNA-damage responses and clinical outcomes.

A druggable p53 pathway gene with cancer risk SNPs associates with pathway inhibitory traits

Various therapeutic efforts have been designed around restoring wild-type p53 activity to improve p53-mediated cell killing (32). The identification of a p53 regulatory cancer risk SNP that affects, in tumors, *TP53* expression levels, activity, *TP53* mutational status, tumor progression, outcome, and radiation responses [as demonstrated for the p53 poly(A) SNP] points to other potential entry points for therapeutically manipulating p53 activities guided by these commonly inherited cancer risk variants. We reasoned that p53 pathway genes with alleles, which increase expression of genes that inhibit p53 cell-killing activities and increase cancer risk, would be potential drug targets to reactivate p53 through their inhibition.

In total, there are 1,133 GWAS implicated cancer-risk SNPs (lead SNPs and proxies) in 41 of 410 annotated p53 pathway genes (Kyoto Encyclopedia of Genes and Genomes,

BioCarta, and PANTHER and/or direct p53 target genes; ref. 33; Fig. 3C; Supplementary Table S7). To systematically identify those p53 pathway genes with cancer risk SNPs whose increased expression associates with inhibition of p53-mediated cancer cell killing, we looked to the above-described drug sensitivity dataset with both somatic genetic and gene expression data (34). In total, the transcript levels of 3 of the 41 p53 pathway genes that harbor cancer risk SNPs associate with Nutlin3 (the most significant compound associated with *wtTP53* CNV status) sensitivities in cell lines with *wtTP53* and no copy number loss compared with those with *TP53* mutations (KITLG, CDKN2A, and TEX9; adjusted $P < 0.05$; Fig. 3D). For all three of the significant associations, increased expression of these genes associates with increased resistance to Nutlin3 treatment. To further validate these associations in terms of their dependency on p53 activation and not solely Nutlin3 treatment, we explored similar associations in the three noted DNA-damaging agents (doxorubicin, etoposide, and cisplatin) that demonstrated sensitivities to *TP53* mutational status (Fig. 3B). Only for *KITLG* (Fig. 3E) did increased expression levels associate with increased resistance towards all four agents.

Increased expression of KITLG attenuates p53's anticancer activities

There are multiple significant associations that are consistent with an inhibitory role of increased KITLG expression on p53's anticancer activities in testicular germ cell tumors (TGCT), a cancer type that rarely mutates *TP53*. First, relative to other cancer types, *KITLG* copy gain (GISTIC score ≥1) is highly enriched in *wtTP53* TGCT (3.7-fold, adjusted $P = 2.9e{-}29$; Fig. 4A). Second, the TGCT GWAS risk allele residing in KITLG is enriched in patients with TGCT with *wtTP53* tumors relative to the *wtTP53* tumors of other cancer types (Fig. 4B). Third, patients with elevated expression of *KITLG* in *wtTP53* TGCT progress faster (Fig. 4C). Fourth, the TGCT GWAS risk locus falls within an intron of *KITLG* occupied by p53 in many different cell types and under many different cellular stresses (Supplementary Fig. S2A). This region contains six common SNPs that are in high linkage disequilibrium (LD) in Europeans ($r^2 > 0.95$; red square, Fig. 4D; refs. 35, 36), including a reported polymorphic p53 response element (p53 RE SNP, rs4590952). The major alleles of this SNP associate with increased TGCT risk, increased p53 binding, transcriptional enhancer activity, and greater *KITLG* expression in heterozygous cancer cell lines wild-type for *TP53* (37). Third, higher grade, but not lower grade, patients with *wtTP53* TGCT carrying alleles associated with increased risk and *KITLG* expression also progress faster (Fig. 4E; Supplementary Figs. S2B and S2C; Supplementary Table S8).

To experimentally test the potential inhibitory role of increased *KITLG* expression on p53's anticancer activities in TGCT, we deleted the risk locus in two TGCT-derived cell lines (TERA1 and TERA2) with *wtTP53* and homozygous for the TGCT risk alleles (p53-REs$^{+/+}$; Fig. 4F; Supplementary Figs. S3A–S3C). As predicted from the above-described associations, we found significantly higher *KITLG* RNA levels in nonedited p53-REs$^{+/+}$ clones, compared with either the heterozygous knockouts (KO) p53-REs clones or the homozygous KOs REs$^{-/-}$ clones (Fig. 4G). After Nutlin3 treatment, the p53-REs$^{-/-}$ clones showed no measurable induction of *KITLG* relative to p53-RE$^{+/+}$ cells (Fig. 4H, red bars vs. gray bars). We found no significant differences between the p53-REs$^{-/-}$ and p53-REs$^{+/+}$ clones in other genes surrounding *KITLG* (±1Mbp; Supplementary Fig. S3D).

Reintegration of the deleted regions into its original locus rescued basal expression, resulting in significantly higher *KITLG* RNA levels in the knock-in (KI) clones of both cell lines relative to the p53-REs$^{-/-}$ (Fig. 4F and I; Supplementary Figs. S3E–S3G). The KI clones also rescued the p53-dependent induction of *KITLG* expression relative to the p53-REs$^{-/-}$ (Fig. 4I).

KITLG is best known to act through the c-KIT receptor tyrosine kinase to promote cell survival in many cancer types (38). To determine if heightened *KITLG*/c-KIT signaling inhibits p53's anticancer activities in TGCT, we explored its impact on cellular sensitivities to p53-activating agents. We found that deletion of the KITLG risk locus or c-KIT knockdown resulted in an increased sensitivity to Nutlin3, and increased levels of cleaved caspase-3 and PARP1 (Fig. 5A and B; Supplementary Figs. S4A and S4B). We were able to rescue the increased Nutlin3 sensitivity and caspase-3/PARP1 cleavage of p53RE$^{-/-}$ clones in KI cells (Fig. 5A; Supplementary Fig. S4C). To further test the p53-dependence of these effects, we reduced *TP53* expression levels and observed reduced expression of cleaved caspase-3 after Nutlin3 treatment (Supplementary Fig. S4D), and an overall insensitivity towards Nutlin3 in both p53-REs$^{+/+}$ and p53-REs$^{-/-}$ cells (Supplementary Fig. S4E).

Thus far, we have demonstrated that TGCT cells with increased expression of *KITLG* have increased procancer survival traits previously attributed to KITLG/cKIT signaling in other cancer types. Moreover, these cells also have traits that suggest an inhibitory effect of KITLG on a p53-associated anticancer activity, namely the apoptotic response to p53 activation after MDM2 inhibition with Nutlin3 treatment. To further explore this, we screened 317 anticancer compounds to identify agents that, like Nutlin3, kill significantly more cells at lower concentrations in p53-RE$^{-/-}$ clones than in p53$^{+/+}$ clones (Fig. 5C). We identified 198 compounds in the TERA1 screen and 112 compounds in the TERA2 screen that showed heightened sensitivity in p53-RE$^{-/-}$ cells in at least one of the four different concentrations tested (≥1.5-fold in both replicates; Supplementary Fig. S5A, blue dots). One hundred of these agents overlapped between TERA1 and TERA2 (1.7-fold, P = 1.1e–21; Supplementary Fig. S5A), suggesting a potential shared mechanism underling the differential sensitivities. For example, two *MDM2* inhibitors in the panel of compounds, Nutlin3 and Serdemetan, were among the 100 overlapping agents (Fig. 5D; Supplementary Table S3). We found a significant and consistent enrichment of topoisomerase inhibitors in both cell lines among 14 different compound classes [14 compounds in TERA1 (100%) and 10 compounds in TERA2 (71%) of 14 Topo inhibitors screened; Fig. 5D and E]. To validate the genotype-specific effects of the topoisomerase inhibitors, we determined the IC_{50} values of three of them (doxorubicin, camptothecin, and topotecan) using MTT measurements in multiple clones of TERA1 cells with differing genotypes. All three agents showed a significant reduction of IC_{50} values, increased sensitivities, in the p53-REs$^{-/-}$ clones (lower KITLG) relative to the p53-REs$^{+/+}$ clones (higher KITLG; Supplementary Fig. S5B). We were able to rescue this increased sensitivity to topoisomerase inhibitors in the p53RE$^{-/-}$ clones in KI cells (Supplementary Fig. S5B). Together, these results demonstrate that TGCT cell lines with heightened KITLG expression mediated by the risk locus, are less sensitive to 100 agents, most of which are known to activate p53-mediated cell killing.

Inhibition of KITLG/c-KIT signaling and p53 activation interact to kill treatment-resistant cancer cells

There are many RTK inhibitors that are current therapeutic agents, which inhibit c-KIT activity (39). If p53-mediated *KITLG*-dependent prosurvival signaling can attenuate chemosensitivity to p53-activating agents, RTK inhibitors should be able to interact synergistically with p53-activating agents to kill TGCT cells. Indeed, comodulation of these two pathways has shown promise in other cancer types (40–42). We therefore tested which RTK inhibitor (known to inhibit c-KIT) kills TCGT cells most efficiently. Of the five FDA-approved RTKs analyzed, pazopanib, imatinib, nilotinib, suntinib, and dasatinib, the most potent was dasatinib (Supplementary Fig. S5C). To determine potential synergy of RTKs with Nutlin3 in TGCT, we treated cells with dasatinib, and quantitated potential drug–drug interactions by calculating combination indices (CI). We observed clear synergistic interactions (CI <1) between Nutlin3 and dasatinib in both TERA1 and TERA2 p53-REs$^{+/+}$ cells (Fig. 5F, gray bars), and enhanced levels of cleaved caspase-3 and PARP1, relative to single drug treatments without altering p53 stabilization (Supplementary Fig. S5D). Consistent with the requirement of the p53-dependent activation of *KITLG*, no synergy between dasatanib and Nutlin3 was detected in p53-REs$^{-/-}$ cells (CI > 1; Fig. 5F, red bars).

We next explored the interaction between dasatinib and multiple DNA-damaging chemotherapeutics known to activate p53. We focused on the three topoisomerase inhibitors (doxorubicin, camptothecin, and topotecan), as well as cisplatin, a chemotherapeutic agent used to treat TGCT and that induces DNA damage and p53. Dasatinib demonstrated significant levels of synergy with each of the DNA-damaging agents tested in p53-REs$^{+/+}$ cells (Supplementary Figs. S5E and S5F). Similar to Nutlin3, no synergy was detected in p53-REs$^{-/-}$ cells of either cell lines for any combination of agents (Supplementary Figs. S5E and S5F). Furthermore, the synergistic interaction between dasatinib and the p53-activating agents Nutlin3 and doxorubin could be rescued by knocking in the p53-bound germline TGCT-risk locus in *KITLG* (Fig. 5G, orange bars).

Thus, a more effective therapeutic strategy for patients with TGCT could be to modulate both the cell death and cell survival functions of p53, through coinhibition of p53/*KITLG*-mediated prosurvival signaling together with the coactivation of p53-mediated antisurvival signaling. Such a therapeutic combination could provide an alternative for patients with treatment-resistant disease (43). To investigate this idea, we explored synergistic interactions between c-KIT inhibitor dasatinib and p53 activators in cisplatin-resistant clones of GCT27 (GCT27-CR) and Susa (Susa-CR; ref. 44), as well as in the intrinsically cisplatin-resistant TGCT cell line 2102EP (45) with *wtTP53* and at least one copy of the haplotype containing the KITLG risk allele SNPs. Similar to the observations in the cisplatin-sensitive TGCT cell lines, dasatinib and doxorubicin interacted synergistically to kill all three cisplatin-resistant clones and cell lines (Fig. 5H). Moreover, cotreat- ment with dasatinib and doxorubicin of Susa-CR and 2102EP led to a significant reduction (~20-fold, on average) in the concentrations of dasatinib and doxorubicin used to achieve IC_{50} relative to when the drugs are used individually (Supplementary Fig. S5G). To determine if the combination treatment could show a greater efficacy in treating tumors, we generated a subcutaneous xenograft model using the 2102EP cell line, and treated the mice with two approved drugs dasatinib

and doxorubicin either alone or in combination. Consistent with the observations made in cell culture, treatment of mice engrafted with 2102EP cells revealed stronger antitumoral effects with the dasatinib/doxorubicin pair relative to single drug treatments (Fig. 5I). This dosing regimen was well tolerated with no body weight loss in mice (Supplementary Fig. S5H).

KITLG/c-KIT signaling interacts with p53 to affect cancer progression and drug response in melanoma

Our results clearly support a model, whereby increased expression of *KITLG* mediated by the region with the TGCT cancer risk SNP(s) heightens KITLG/c-KIT signaling and attenuates p53 activity, thereby allowing for the retention and reactivation of *wtTP53* in testicular cancer cells. The *KITLG* testicular cancer risk SNP(s) have yet to be found to associate with other cancer types (46), suggesting a tissue-specificity of this locus with transcriptional enhancer activity. However, other genetic variants that elevate KITLG/c-KIT signaling could also attenuate p53 activity, and thus allow for the retention and ultimate reactivation of *wtTP53* in cancer cells. To test this, we focused on known somatic driver mutations of *c-KIT* in the TCGA cohort. If our model is correct, we would expect the majority of tumors with activating *c-KIT* mutations to retain a *wtTP53* locus. Indeed, 43 of 6,997 (0.61%) patients with *wtTP53* tumors also have oncogenic *c-KIT* mutations relative to just 10 of 3,735 (0.27%) of *TP53* mutant tumors (Fig. 6A; OR = 2.3; $P = 0.014$).

As expected, the tumor types enriched in c-KIT oncogenic mutations in the TCGA cohort are cancers known to be driven by KIT signaling (38). Testicular cancers (TGCT; 13.6%; 20 of 147), skin cutaneous melanoma (SKCM; 3.9%; 14 of 356), and acute myeloid leukemias (AML; 2.8%; 5 of 181) have proportionally more *c-KIT* mutations than all *wtTP53* tumors (0.61%; $P_{adj} < 0.05$; Fig. 6B, left). It is important to note that these enrichments are only significant when *wtTP53* without *TP53*-loss, but not *TP53* loss or mutant tumors are considered (Fig. 6B). If our model is correct and inhibition of c-KIT signaling will reactivate p53's ability to kill the *wtTP53* cancers, we would expect, like in TGCT, that elevated *KITLG* levels will associate with faster progression and/or poorer survival of the cancers with both wild-type *TP53* and *c-KIT*. Indeed, in both melanoma and AML, we observed the association between heightened *KITLG* expression and poorer clinical outcomes (Fig. 6C, the TCGA-SKCM cohort; Fig. 6D, the TCGA-AML cohort). Consistent associations were observed in an independent cohort (DFCI-SKCM) of 35 patients with *wtTP53* melanoma (Fig. 6E), for which both the somatic genetic and expression data are available (47). Importantly, we found that in patients with melanoma and AML with *wtTP53* and no copy number loss tumors, those with heightened *KITLG* expression have significantly poorer outcomes, but not in patients with *TP53* mutant or copy number loss (Fig. 6F and G). Together these observations, suggest that heightened KITLG/cKIT signaling in AML and melanoma could attenuate p53 activity allowing for wt *TP53* retention and reactivation using cKIT inhibitors. In further support of this, in AML, it has been shown that the c-Kit inhibitor dasatinib does enhance p53-mediated cell killing (40). Similarly, when we treated melanoma cells (SKMEL5 with wild-type *TP53* and *c-KIT*) with dasatinib and the p53-activating agents Nutlin3 or doxorubicin, we observed clear synergistic interactions (Fig. 6H, CI <

1; $P = 0.0013$ between Nutlin3 and dasatinib and $P = 0.00066$ between doxorubicin and dasatinib).

Discussion

In this study, we demonstrate that germline cancer-risk SNPs could inf1uence cancer progression and potentially provide information guiding precision medicine therapy decisions. Our work highlights that even small relative reductions in *wtTP53* expression, mediated either by the minor allele of the p53 poly(A) SNP or through loss of at least one copy of *TP53*, can reduce relative p53 cellular activity in cancer cells and overall survival of patients. Patients with either of these genetic variations represent a large proportion of patients with cancer. Patients with the minor allele of the SNP and *wtTP53* in their cancers are found in 2.6% of the total TCGA cohort, with up to 5.9% in certain cancer types. Overall, in the TCGA, 26.6% of patients have cancers wherein at least one copy of *wtTP53* is lossed with up to 73.1% in certain cancer types. In terms of including *TP53* status in prognosis for patients, *TP53* mutation is often what is looked at most. Our work suggests that *wtTP53* copy number loss could also add additional information to those patients that retain *wtTP53*. Indeed, patients with tumors that express lower *wtTP53* levels will be interesting to study more in depth to understand how to increase *wtTP53* levels to improve treatments, such as increasing transcription of *wtTP53*, inhibiting miRNAs or blocking alternative polyadenylation.

The p53 stress response pathway inhibits cell survival, mediating both tumor suppression and cellular responses to many cancer therapeutics (48). p53 also targets prosurvival genes. Activation of these genes in tumors retaining *wtTP53* provide a survival advantage (49). We provide human genetic evidence that also supports a tumor-promoting role of p53 prosurvival activities and, in the case of the TGCT risk locus, points to the development of more effective therapy combinations through the inhibition of these prosurvival activities in tumors that retain p53 activity. Although TGCTs are one of the most curable solid tumors, men diagnosed with metastatic TGCT develop platinum-resistant disease and die at an average age of 32 years (43). There have been few new treatments developed in the last two decades, and current therapeutic approaches can, importantly in context of a cancer of young men, result in significant survivorship issues, including sustained morbidities and delayed major sequelae (43). Our observations suggest the TGCT *KITLG* risk allele in the polymorphic p53 enhancer leads to increased p53-dependent activation of the prosurvival target gene, *KITLG*, which increases TGCT survival rather than senescence/apoptosis in the presence of active p53. We demonstrate that coinhibition of c-KIT and p53 activation interact synergistically to kill platinum-resistant TGCTs with a drug combination (dasatinib and doxorubicin) that had limited toxicity in a Phase II clinical trial (50), suggesting that an effective therapeutic strategy for treatment-resistant TGCTs could be to modulate both the cell-death and cell-survival functions of *wtTP53* cancers.

Using the most well-studied somatic mutation known to enhance KITLG/c-KIT signaling (*c-KIT* mutations), we were able to identify SKCM as another potential repurposing opportunity for combination therapies, which inhibit KITLG/c-KIT signaling and activate p53. The role of c-KIT signaling in the skin is well established with the pathway of

crucial importance for the development of melanocytes (51). In line with previous work, we found *wtTP53* SKCM to be enriched for c-KIT mutations (52, 53). Furthermore, we found high *KITLG* expression to associate independently with poorer overall survival in patients with *wtTP53* SKCM. Our data provide molecular support for targeting of KITLG/c-KIT in melanoma. Melanoma rarely mutates *TP53* and expresses high levels of p53 protein, in line with the fact that SKCM is enriched for *wtTP53* and no *TP53* copy number loss (54). Melanomas are hardwired to be resistant to p53-dependent apoptosis, perhaps because melanocytes are programmed to survive UV light (55). Several mechanisms have been proposed for this inhibition of p53 triggered apoptosis, including the action of iASPP, deletion of the CDKN2A locus, aberrant phosphorylation of p53, and activation of MDM2 by downstream c-KIT signaling (55, 56). More recently, it has been shown that WNT5a signaling and wild-type p53 might cooperate in melanoma to drive cells into a slow cycling state, which is therapy resistant (57). It is possible that KITLG/c-KIT-mediated inhibition of the p53-apoptotic response adds a further mechanism through which *wtTP53* can be inhibited in melanoma without mutation, and opens up the possibility of harnessing the proapoptotic function of p53 by inhibiting the KITLG/c-KIT pathway. Indeed, we showed that the combination of dasatinib and Nutlin-3a and dasatinib and doxorubicin are synergistic in a wild-type *TP53* and *c-KIT* SKCM cell-line.

Unlike other tumor suppressors, complete loss of p53 activity is not a requirement for cancer initiation. Reduction of p53 activity below a critical threshold through mutations is apparently necessary and sufficient for cancer development (58). These mutations are primarily missense mutations that affect p53's ability to bind to DNA in a sequence-specific manner and regulate transcription of its target genes. These same mutations when found constitutionally result in Li-Fraumeni Syndrome: a syndrome comprising dramatic increase in cancer risk in many tissues types. These missense mutations may benefit cancers not simply through loss of p53 function, but also through dominant-negative and gain-of-function activities (59). In mice, KI *TP53* gain-of-function mutants displayed a more diverse set of, and more highly metastatic tumors than *TP53* knockout mutants (60, 61). Many of the factors that regulate wild-type p53 tumor suppression can also regulate mutant p53, including its procancer activities. For example, wild-type p53 mice that express lower levels of MDM2 show increased p53 levels, a better p53 stress response, and greater tumor suppression, resulting in later and reduced tumor onset in many tissue types. Mutant p53 levels are also increased in these murine models, but cancers are found to arise earlier and harbor gain-of-function metastatic phenotypes (62).

We go on to discuss that our SNP association with inverted cancer risk and somatic *TP53* mutational status in humans reveal a similar scenario. Specifically, we demonstrated that the C-allele of the p53 poly(A) SNP, which can lead to decreased wild-type and mutant p53 levels in tumors, associates with an increased risk of *wtTP53* cancers, but decreased risk of subtypes with primarily mutant *TP53*. For example, women with the minor allele associated with an increased risk for the more *TP53* wild-type breast and ovarian subtypes and a decreased risk for the more mutant subtypes. We also demonstrated that the patients with TCGA pan-cancer or breast cancer with *wtTP53* tumors and carrying the C allele have shorter PFI compared with patients with *wtTP53* tumors without the C allele. Of note, an inverted trend was found for mutant *TP53* tumors. Together, these observations support a

role for germline p53 pathway SNPs not only in modulating risk of disease and tumor biology in *wtTP53* cancers but also in *TP53* mutant cancers, wherein alleles that increase mutant p53 levels would also increase its procancer activities.

Supplementary Material

Refer to Web version on PubMed Central for supplementary material.

Acknowledgments

This work was funded in part by the Ludwig Institute for Cancer Research, the Nuffield Department of Medicine, the Development Fund, Oxford Cancer Research Centre, University of Oxford, UK, by the Intramural Research Program of the National Institute of Environmental Health Sciences-National Institutes of Health (Z01-ES100475), and NIH grant (DP5-OD017937), US, and by the S-CORT Consortium from the Medical Research Council and Cancer Research UK.

Authors' Disclosures

J. Zeron-Medina reports employment with AstraZeneca. S.P. Blagden reports grants from Nucana PLC and other funding from Redx, Sierra Oncology, Astex, Incyte, Octimet, and Tesaro outside the submitted work. T.S. Maughan reports grants from AstraZeneca, Merck Serono, and PsiOxus; personal fees from AstraZeneca and Pierre Fabre; and nonfinancial support from AstraZeneca, Merck Serono, and PsiOxus outside the submitted work; and has a patent for patent pending. H. Carter reports grants from NIH, The Mark Foundation for Cancer Research, and Harry J. Lloyd Charitable Trust during the conduct of the study. No other disclosures were reported by the other authors.

References

1. Dancey JE, Bedard PL, Onetto N, Hudson TJ. The genetic basis for cancer treatment decisions. Cell 2012;148:409–20. [PubMed: 22304912]
2. Huang M, Shen A, Ding J, Geng M. Molecularly targeted cancer therapy: some lessons from the past decade. Trends Pharmacol Sci 2014;35:41–50. [PubMed: 24361003]
3. Carter H, Marty R, Hofree M, Gross AM, Jensen J, Fisch KM, et al. Interaction landscape of inherited polymorphisms with somatic events in cancer. Cancer Discov 2017;7:410–23. [PubMed: 28188128]
4. Lu C, Xie M, Wendl MC, Wang J, McLellan MD, Leiserson MD, et al. Patterns and functional implications of rare germline variants across 12 cancer types. Nat Commun 2015;6:10086.
5. Yurgelun MB, Chenevix-Trench G, Lippman SM. Translating germline cancer risk into precision prevention. Cell 2017;168:566–70. [PubMed: 28187278]
6. Stracquadanio G, Wang XT, Wallace MD, Grawenda AM, Zhang P, Hewitt J, et al. The importance of p53 pathway genetics in inherited and somatic cancer genomes. Nat Rev Cancer 2016;16:251–65. [PubMed: 27009395]
7. Martincorena I, Raine KM, Gerstung M, Dawson KJ, Haase K, Van Loo P, et al. Universal patterns of selection in cancer and somatic tissues. Cell 2017;171:1029–41. [PubMed: 29056346]
8. Kastenhuber ER, Lowe SW. Putting p53 in context. Cell 2017;170:1062–78. [PubMed: 28886379]
9. Bouwman P, Jonkers J. The effects of deregulated DNA damage signalling on cancer chemotherapy response and resistance. Nat Rev Cancer 2012;12:587–98. [PubMed: 22918414]
10. Lowe SW, Ruley HE, Jacks T, Housman DE. P53-dependent apoptosis modulates the cytotoxicity of anticancer agents. Cell 1993;74:957–67. [PubMed: 8402885]
11. Weinstein JN, Myers TG, O'Connor PM, Friend SH, Fornace AJ Jr, Kohn KW, et al. An information-intensive approach to the molecular pharmacology of cancer. Science 1997;275:343–9. [PubMed: 8994024]
12. Willer CJ, Li Y, Abecasis GR. METAL: fast and efficient meta-analysis of genomewide association scans. Bioinformatics 2010;26:2190–1. [PubMed: 20616382]

13. Liu JF, Lichtenberg T, Hoadley KA, Poisson LM, Lazar AJ, Cherniack AD, et al. An integrated TCGA pan-cancer clinical data resource to drive high-quality survival outcome analytics. Cell 2018;173:400–16. [PubMed: 29625055]
14. Ran FA, Hsu PD, Wright J, Agarwala V, Scott DA, Zhang F. Genome engineering using the CRISPR-Cas9 system. Nat Protoc 2013;8:2281–308. [PubMed: 24157548]
15. Zhang P, Elabd S, Hammer S, Solozobova V, Yan H, Bartel F, et al. TRIM25 has a dual function in the p53/Mdm2 circuit. Oncogene 2015;34:5729–38. [PubMed: 25728675]
16. Chou TC. Theoretical basis, experimental design, and computerized simulation of synergism and antagonism in drug combination studies. Pharmacol Rev 2006; 58:621–81. [PubMed: 16968952]
17. Stacey SN, Sulem P, Jonasdottir A, Masson G, Gudmundsson J, Gudbjartsson DF, et al. A germline variant in the TP53 polyadenylation signal confers cancer susceptibility. Nat Genet 2011;43:1098–103. [PubMed: 21946351]
18. Consortium GT. The genotype-tissue expression (GTEx) project. Nat Genet 2013;45:580–5. [PubMed: 23715323]
19. Deng Q, Hu H, Yu X, Liu S, Wang L, Chen W, et al. Tissue-specific microRNA expression alters cancer susceptibility conferred by a TP53 noncoding variant. Nat Commun 2019;10:5061. [PubMed: 31699989]
20. Rafnar T, Gunnarsson B, Stefansson OA, Sulem P, Ingason A, Frigge ML, et al. Variants associating with uterine leiomyoma highlight genetic background shared by various cancers and hormone-related traits. Nat Commun 2018; 9:3636. [PubMed: 30194396]
21. Zhang H, Ahearn TU, Lecarpentier J, Barnes D, Beesley J, Qi G, et al. Genome-wide association study identifies 32 novel breast cancer susceptibility loci from overall and subtype-specific analyses. Nat Genet 2020;52:572–81. [PubMed: 32424353]
22. Landi MT, Bishop DT, MacGregor S, Machiela MJ, Stratigos AJ, Ghiorzo P, et al. Genome-wide association meta-analyses combining multiple risk phenotypes provide insights into the genetic architecture of cutaneous melanoma susceptibility. Nat Genet 2020;52:494–504. [PubMed: 32341527]
23. Rashkin SR, Graff RE, Kachuri L, Thai KK, Alexeeff SE, Blatchins MA, et al. Pan-cancer study detects genetic risk variants and shared genetic basis in two large cohorts. Nat Commun 2020;11:4423. [PubMed: 32887889]
24. Cancer Genome Atlas Network. Comprehensive molecular portraits of human breast tumours. Nature 2012;490:61–70. [PubMed: 23000897]
25. Cancer Genome Atlas Research Network. Integrated genomic analyses of ovarian carcinoma. Nature 2011;474:609–15. [PubMed: 21720365]
26. Michailidou K, Lindstrom S, Dennis J, Beesley J, Hui S, Kar S, et al. Association analysis identifies 65 new breast cancer risk loci. Nature 2017;551:92–4. [PubMed: 29059683]
27. Phelan CM, Kuchenbaecker KB, Tyrer JP, Kar SP, Lawrenson K, Winham SJ, et al. Identification of 12 new susceptibility loci for different histotypes of epithelial ovarian cancer. Nat Genet 2017;49:680–91. [PubMed: 28346442]
28. Suh YA, Post SM, Elizondo-Fraire AC, Maccio DR, Jackson JG, El-Naggar AK, et al. Multiple stress signals activate mutant p53 in vivo. Cancer Res 2011;71:7168–75. [PubMed: 21983037]
29. Yue X, Zhao Y, Xu Y, Zheng M, Feng Z, Hu W. Mutant p53 in cancer: accumulation, gain-of-function, and therapy. J Mol Biol 2017;429:1595–606. [PubMed: 28390900]
30. Burckstummer T, Banning C, Hainzl P, Schobesberger R, Kerzendorfer C, Pauler FM, et al. A reversible gene trap collection empowers haploid genetics in human cells. Nat Methods 2013;10:965–71. [PubMed: 24161985]
31. Gudkov AV, Komarova EA. The role of p53 in determining sensitivity to radiotherapy. Nat Rev Cancer 2003;3:117–29. [PubMed: 12563311]
32. Hientz K, Mohr A, Bhakta-Guha D, Efferth T. The role of p53 in cancer drug resistance and targeted chemotherapy. Oncotarget 2017;8:8921–46. [PubMed: 27888811]
33. Census Fischer M. and evaluation of p53 target genes. Oncogene 2017;36:3943–56. [PubMed: 28288132]
34. Iorio F, Knijnenburg TA, Vis DJ, Bignell GR, Menden MP, Schubert M, et al. A landscape of pharmacogenomic interactions in cancer. Cell 2016; 166:740–54. [PubMed: 27397505]

35. Turnbull C, Rapley EA, Seal S, Pernet D, Renwick A, Hughes D, et al. Variants near DMRT1, TERT and ATF7IP are associated with testicular germ cell cancer. Nat Genet 2010;42:604–U178. [PubMed: 20543847]
36. Litchfield K, Levy M, Orlando G, Loveday C, Law PJ, Migliorini G, et al. Identification of 19 new risk loci and potential regulatory mechanisms inf1uencing susceptibility to testicular germ cell tumor. Nat Genet 2017; 49:1133–1140. [PubMed: 28604728]
37. Zeron-Medina J, Wang X, Repapi E, Campbell MR, Su D, Castro-Giner F, et al. A polymorphic p53 response element in KIT ligand inf1uences cancer risk and has undergone natural selection. Cell 2013;155:410–22. [PubMed: 24120139]
38. Lennartsson J, Ronnstrand L. Stem cell factor receptor/c-Kit: from basic science to clinical implications. Physiol Rev 2012;92:1619–49. [PubMed: 23073628]
39. Flaherty KT, Hodi FS, Fisher DE. From genes to drugs: targeted strategies for melanoma. Nat Rev Cancer 2012;12:349–61. [PubMed: 22475929]
40. Dos Santos C, McDonald T, Ho YW, Liu H, Lin A, Forman SJ, et al. The Src and c-Kit kinase inhibitor dasatinib enhances p53-mediated targeting of human acute myeloid leukemia stem cells by chemotherapeutic agents. Blood 2013;122:1900–13. [PubMed: 23896410]
41. Henze J, Muhlenberg T, Simon S, Grabellus F, Rubin B, Taeger G, et al. p53 modulation as a therapeutic strategy in gastrointestinal stromal tumors. PLoS One 2012;7:e37776.
42. Kurosu T, Wu N, Oshikawa G, Kagechika H, Miura O. Enhancement of imatinib-induced apoptosis of BCR/ABL-expressing cells by nutlin-3 through synergistic activation of the mitochondrial apoptotic pathway. Apoptosis 2010; 15:608–20. [PubMed: 20094798]
43. Litchfield K, Levy M, Huddart RA, Shipley J, Turnbull C. The genomic landscape of testicular germ cell tumours: from susceptibility to treatment. Nat Rev Urol 2016;13:409–19. [PubMed: 27296647]
44. Noel EE, Yeste-Velasco M, Mao X, Perry J, Kudahetti SC, Li NF, et al. The association of CCND1 overexpression and cisplatin resistance in testicular germ cell tumors and other cancers. Am J Pathol 2010;176:2607–15. [PubMed: 20395447]
45. Koster R, di Pietro A, Timmer-Bosscha H, Gibcus JH, van den Berg A, Suurmeijer AJ, et al. Cytoplasmic p21 expression levels determine cisplatin resistance in human testicular cancer. J Clin Invest 2010;120:3594–605. [PubMed: 20811155]
46. Buniello A, MacArthur JAL, Cerezo M, Harris LW, Hayhurst J, Malangone C, et al. The NHGRI-EBI GWAS Catalog of published genome-wide association studies, targeted arrays and summary statistics 2019. Nucleic Acids Res 2019;47:D1005–D12.
47. Van Allen EM, Miao D, Schilling B, Shukla SA, Blank C, Zimmer L, et al. Genomic correlates of response to CTLA-4 blockade in metastatic melanoma. Science 2015;350:207–11. [PubMed: 26359337]
48. Vazquez A, Bond EE, Levine AJ, Bond GL. The genetics of the p53 pathway, apoptosis and cancer therapy. Nat Rev Drug Discov 2008;7:979–87. [PubMed: 19043449]
49. Kruiswijk F, Labuschagne CF, Vousden KH. p53 in survival, death and metabolic health: a lifeguard with a licence to kill. Nat Rev Mol Cell Bio 2015; 16:393–405. [PubMed: 26122615]
50. Benjamini O, Dumlao TL, Kantarjian H, O'Brien S, Garcia-Manero G, Faderl S, et al. Phase II trial of HyperCVAD and Dasatinib in patients with relapsed Philadelphia chromosome positive acute lymphoblastic leukemia or blast phase chronic myeloid leukemia. Am J Hematol 2014; 89:282–7. [PubMed: 24779033]
51. Wehrle-Haller B. The role of Kit-ligand in melanocyte development and epidermal homeostasis. Pigment Cell Res 2003;16:287–96. [PubMed: 12753403]
52. Beadling C, Jacobson-Dunlop E Hodi FS, Le C, Warrick A, Patterson J, et al. . KIT gene mutations and copy number in melanoma subtypes. Clin Cancer Res 2008; 14:6821–8. [PubMed: 18980976]
53. Curtin JA, Busam K, Pinkel D, Bastian BC. Somatic activation of KIT in distinct subtypes of melanoma. J Clin Oncol 2006;24:4340–6. [PubMed: 16908931]
54. McGregor JM, Yu CC, Dublin EA, Barnes DM, Levison DA, MacDonald DM. p53 immunoreactivity in human malignant melanoma and dysplastic naevi. Br J Dermatol 1993;128:606–11. [PubMed: 8338744]

55. Box NF, Vukmer TO, Terzian T. Targeting p53 in melanoma. Pigment Cell Melanoma Res 2014;27:8–10. [PubMed: 24118922]

56. Lu M, Breyssens H, Salter V, Zhong S, Hu Y, Baer C, et al. Restoring p53 function in human melanoma cells by inhibiting MDM2 and cyclin B1/CDK1-phosphorylated nuclear iASPP. Cancer Cell 2013;23:618–33. [PubMed: 23623661]

57. Webster MR, Fane ME, Alicea GM, Basu S, Kossenkov AV, Marino GE, et al. Paradoxical role for wild-type p53 in driving therapy resistance in melanoma. Mol Cell 2020;77:681. [PubMed: 32032511]

58. Hohenstein P. Tumour suppressor genes—one hit can be enough. PLoS Biol 2004;2:E40. [PubMed: 14966536]

59. Muller PA, Vousden KH. Mutant p53 in cancer: new functions and therapeutic opportunities. Cancer Cell 2014;25:304–17. [PubMed: 24651012]

60. Lang GA, Iwakuma T, Suh YA, Liu G, Rao VA, Parant JM, et al. Gain of function of a p53 hot spot mutation in a mouse model of Li-Fraumeni syndrome. Cell 2004;119:861–72. [PubMed: 15607981]

61. Olive KP, Tuveson DA, Ruhe ZC, Yin B, Willis NA, Bronson RT, et al. Mutant p53 gain of function in two mouse models of Li-Fraumeni syndrome. Cell 2004; 119:847–60. [PubMed: 15607980]

62. Terzian T, Suh YA, Iwakuma T, Post SM, Neumann M, Lang GA, et al. The inherent instability of mutant p53 is alleviated by Mdm2 or p16INK4a loss. Genes Dev 2008;22:1337–44. [PubMed: 18483220]

Significance:

These results offer evidence of how cancer susceptibility SNPs can interact with cancer driver genes to affect cancer progression and present novel therapeutic targets.

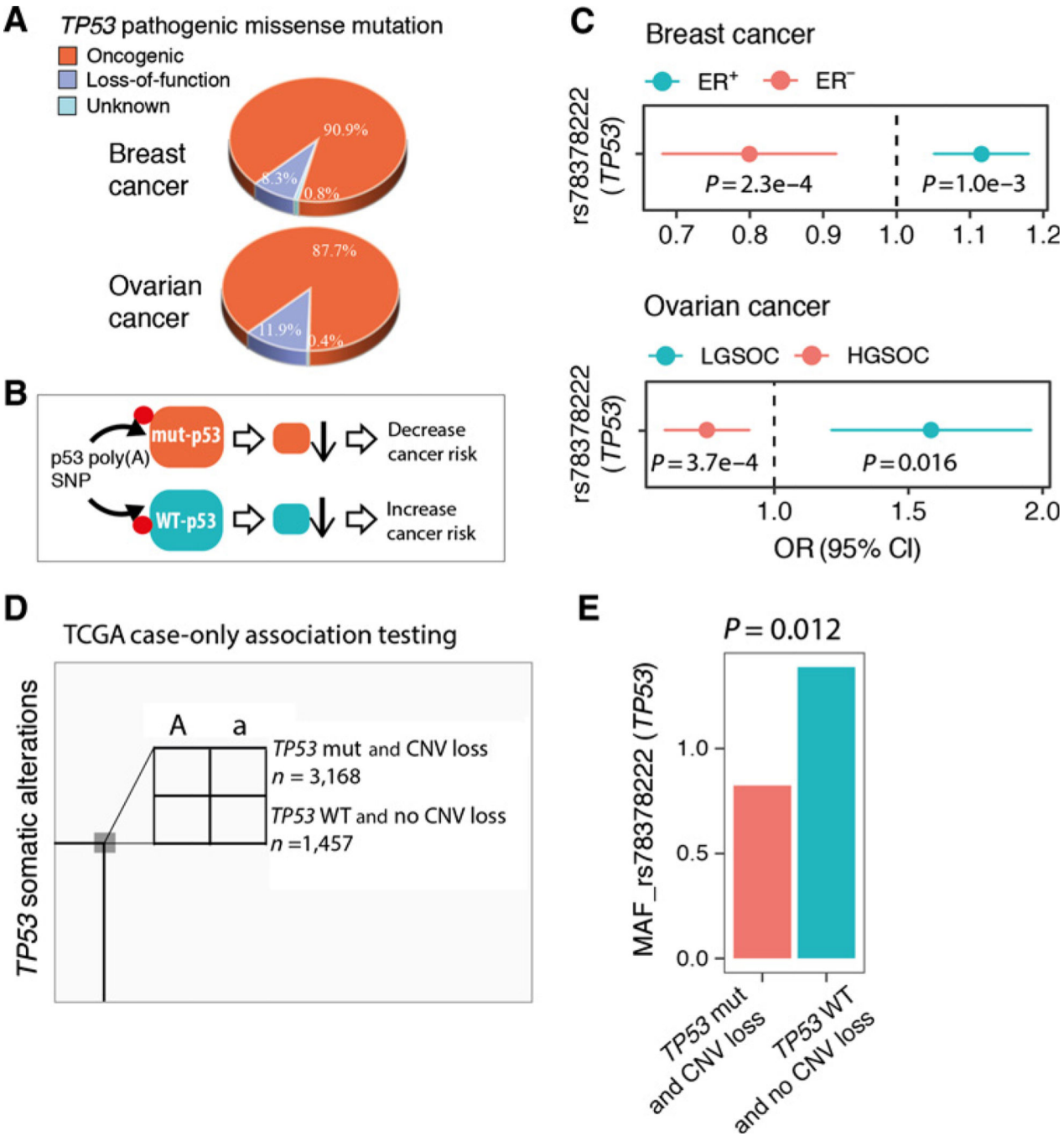

Figure 1.

A p53 regulatory cancer risk SNP associates with subtype heterogeneity risk. **A,** Pie charts of the percentages of oncogenic and loss-of-function *TP53* mutations found amongst all known pathogenic *TP53* missense mutations in breast and ovarian cancers. **B,** A proposed model of how the p53 poly(A) SNP could modify the ability of mutant p53 to drive cancer and of wild-type p53 to suppress it. **C,** Forest plots illustrating the associations of the p53 poly(A) SNP with breast cancer and ovarian cancer subtypes. The ORs are plotted for the SNP and subtype, and the error bars represent the associated 95% CIs. D, A schematic

overview of the association testing between the SNP and *TP53* mutational status in TCGA tumors. **E,** A bar plot of the MAFs of the p53 poly(A) SNP in patients with either *wtTP53* tumors or mutant *TP53* tumors.

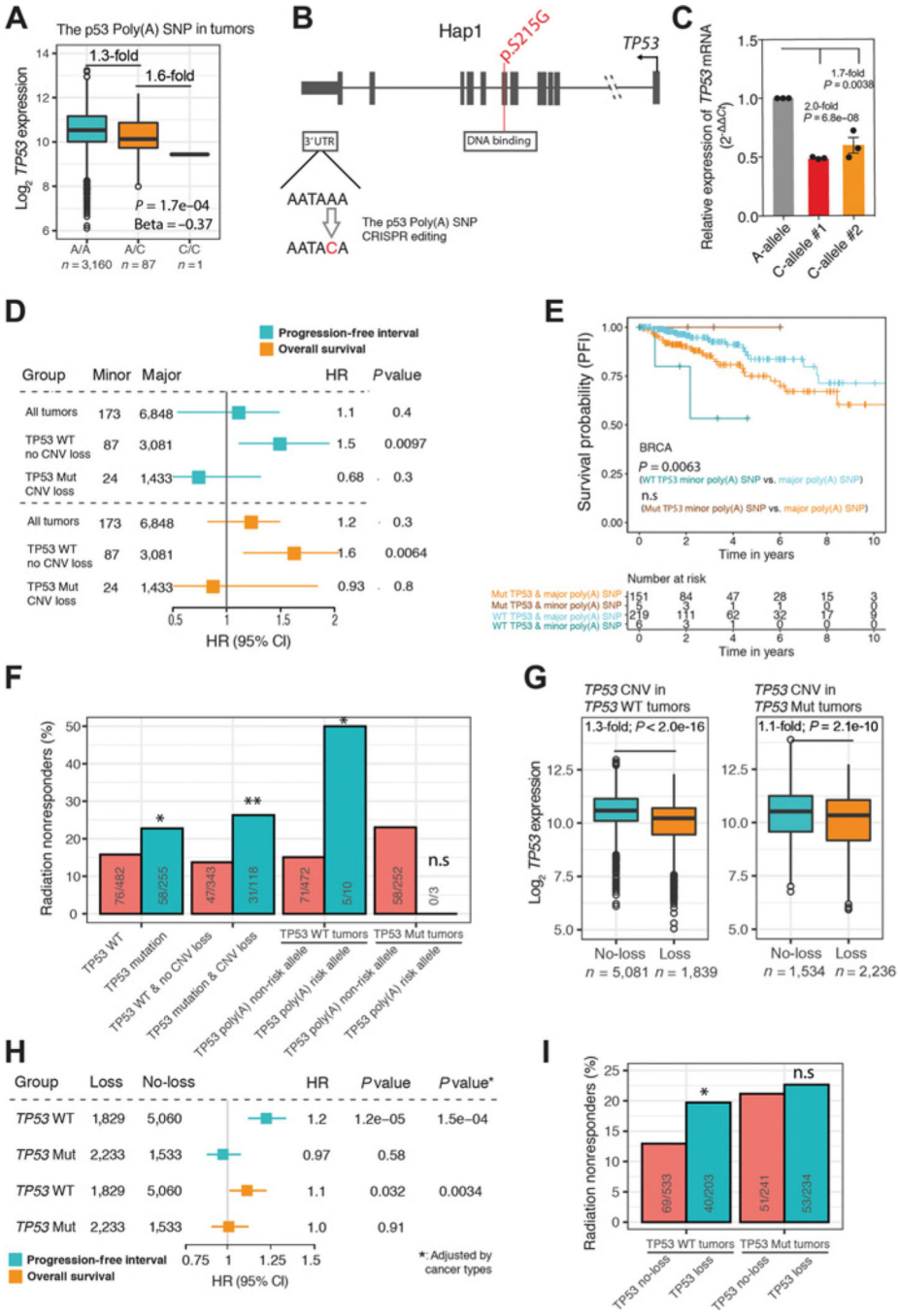

Figure 2.

A p53 regulatory cancer risk SNP and somatic copy number loss of p53 associates with clinical outcomes. **A,** A box plot of *TP53* mRNA expression levels in 3,248 tumors from individuals with differing genotypes of the p53 poly(A) SNP. The fold change of median *TP53* expression between genotypes, and the *P* value (linear regression) and β coefficients of the association of the genotype with mRNA levels are depicted. **B,** A schematic diagram of the *TP53* mutational status and CRISPR-editing strategy in Hap1 cells. **C,** A bar plot of *TP53* mRNA levels for each genotype in Hap1 cells, measured using qRT-PCR normalized

to GAPDH. Error bars represent SEM of three independent experiments. *P* values were calculated using a two-tailed *t* test. **D,** A forest plot of the PFI and OS of patients with cancer (pan-cancer TCGA cohort) stratified by the somatic *TP53* mutational status. HR and *P* values were calculated using Cox proportional hazards model. **E,** Kaplan-Meier survival curves for PFI in a total of 381 patients with breast cancer carrying either the major or the minor allele of the p53 poly(A) SNP and/or somatic *TP53* mutations. Curves were truncated at 10 years, but the statistical analyses were performed using all of the data (log-rank test). **F,** A bar plot showing the percentage of nonresponders in each group stratified by the somatic or germline *TP53* alterations as indicated on the *x*-axis. Numbers of patients (number of nonresponders/total number of patients) in each group are indicated within the bars. *P* values were calculated by two-tailed Fisher exact test.*, $P < 0.05$;**, $P < 0.005$. **G,** Box plots of *TP53* mRNA expression levels in *wtTP53* tumors (left) and mutant *TP53* tumors (right) from individuals with differing *TP53* copy number status. **H,** A forest plot of PFI and OS of TCGA patients with cancer stratified by the somatic *TP53* mutational status. HR comparing PFI and OS in patients with or without *TP53* copy number loss is indicated on the right. **I,** A bar plot showing the percentage of nonresponders in each group stratified by the *TP53* mutations and copy number loss as indicated on the *x*-axis. n.s, no significant.

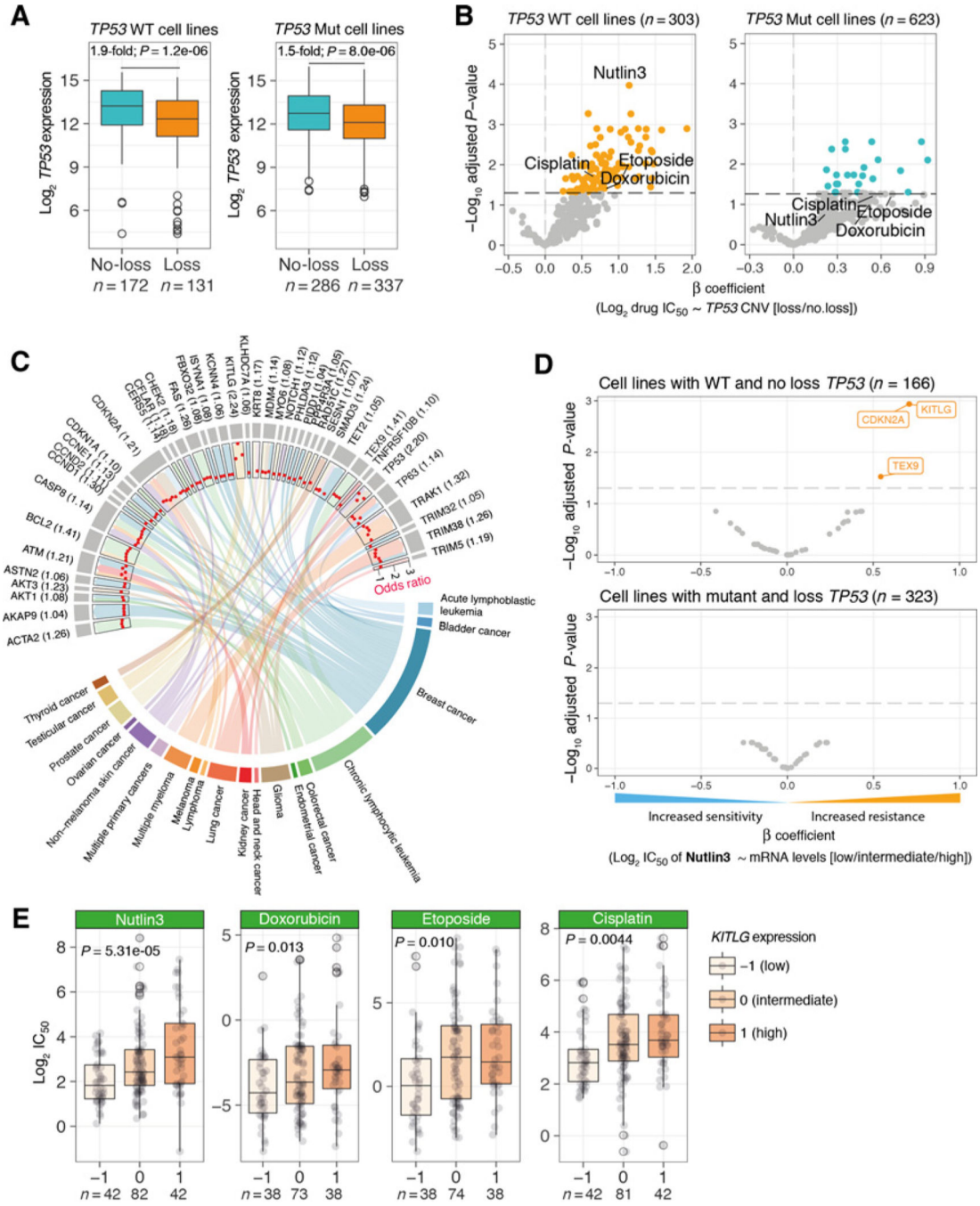

Figure 3.

Copy number loss of *TP53* and increased expression of a druggable pathway gene with cancer risk SNPs dampens p53's anticancer activities. **A,** Box plots of p53 mRNA expression levels in *wtTP53* cells (left) and mutant *TP53* cells (right) with differing *TP53* copy number statuses. **B,** Volcano plots of 304 drugs and their association with differential sensitivities in cancer cell lines with *TP53* copy number loss relative to cell lines without *TP53* copy number loss (left, *wtTP53* cells; right, mutant *TP53* cells). $-\text{Log}_{10}$-adjusted *P* values (linear regression and FDR adjusted) are plotted against the beta coefficient. The

horizontal dashed lines represent the FDR-adjusted *P* value of 0.05. **C,** A chord diagram of 102 cancer GWAS lead SNPs in 41 p53 pathway genes that associate with differential risk to a total of 19 different cancer types. The width of the connecting bands indicate the number of lead SNPs for each association. A dot plot of the odds ratios for each association is presented in the inner circle and with red dots. The median OR for each association is presented in parentheses next to the gene name. **D,** Volcano plots of the associations between the transcript levels of the 41 p53 pathway cancer GWAS genes and Nutlin3 sensitivities in cancer cell lines with either *wtTP53*-no.loss (top) or *TP53* mutant-loss (bottom). **E,** Box plots of the Log_2 IC_{50} values of p53 activating agents in cells either with low, intermediate, or high KITLG mRNA levels and *wtTP53*-no.loss.

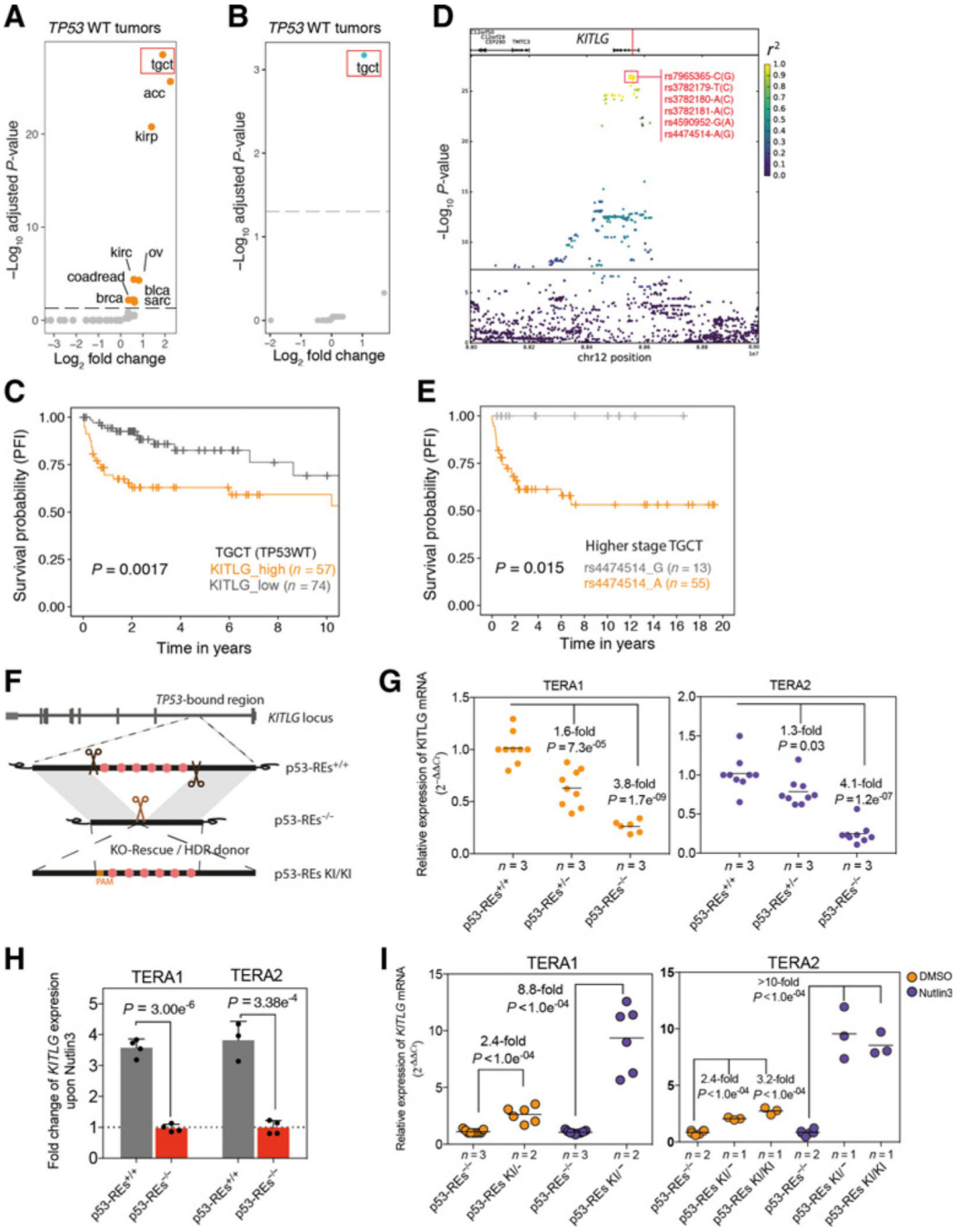

Figure 4.

The p53-bound cancer risk locus in *KITLG* associates with patient outcome and attenuates p53's anticancer activities. **A** and **B,** Dot plots showing the enrichment of *KITLG* copy number gains (**A**) and risk allele frequencies (**B**) across TCGA cancer types. $-\text{Log}_{10}$-adjusted *P* values are plotted against the $\log_2$-fold change of the percentage of tumors with *KITLG* gains/risk alleles in a given cancer type versus the other cancers combined. **C,** A Kaplan–Meier survival curve for PFI in patients with p53wt testicular cancer with high or low *KITLG* mRNA expression. *P* value was calculated using log-rank test. **D,** Genetic fine

mapping identified six SNPs with the strongest TGCT GWAS signal and that are in high linkage disequilibrium (r^2) in Europeans (red square). **E,** A Kaplan–Meier survival curve for PFI in patients with high-stage p53wt testicular cancer carrying either the risk (orange) or the non-risk allele (gray) of the *KITLG* risk SNP. **F,** A diagram of the CRISPR-editing utilized. **G,** *KITLG* gene expression in CRISPR-edited clones using qRT-PCR normalized to GAPDH. In total, two to three clones of each genotype were analyzed in three independent biological replicates. *P* values were calculated using a one-way ANOVA, followed by Tukey multiple comparison test. **H,** A bar graph of the fold change in *KITLG* expression after Nutlin3 treatment. Error bars represent SEM of two clones for each genotype and in two independent experiments. *P* values were calculated using a two-tailed *t* test. **I,** Dot plots of *KITLG* expression in CRISPR-edited clones.

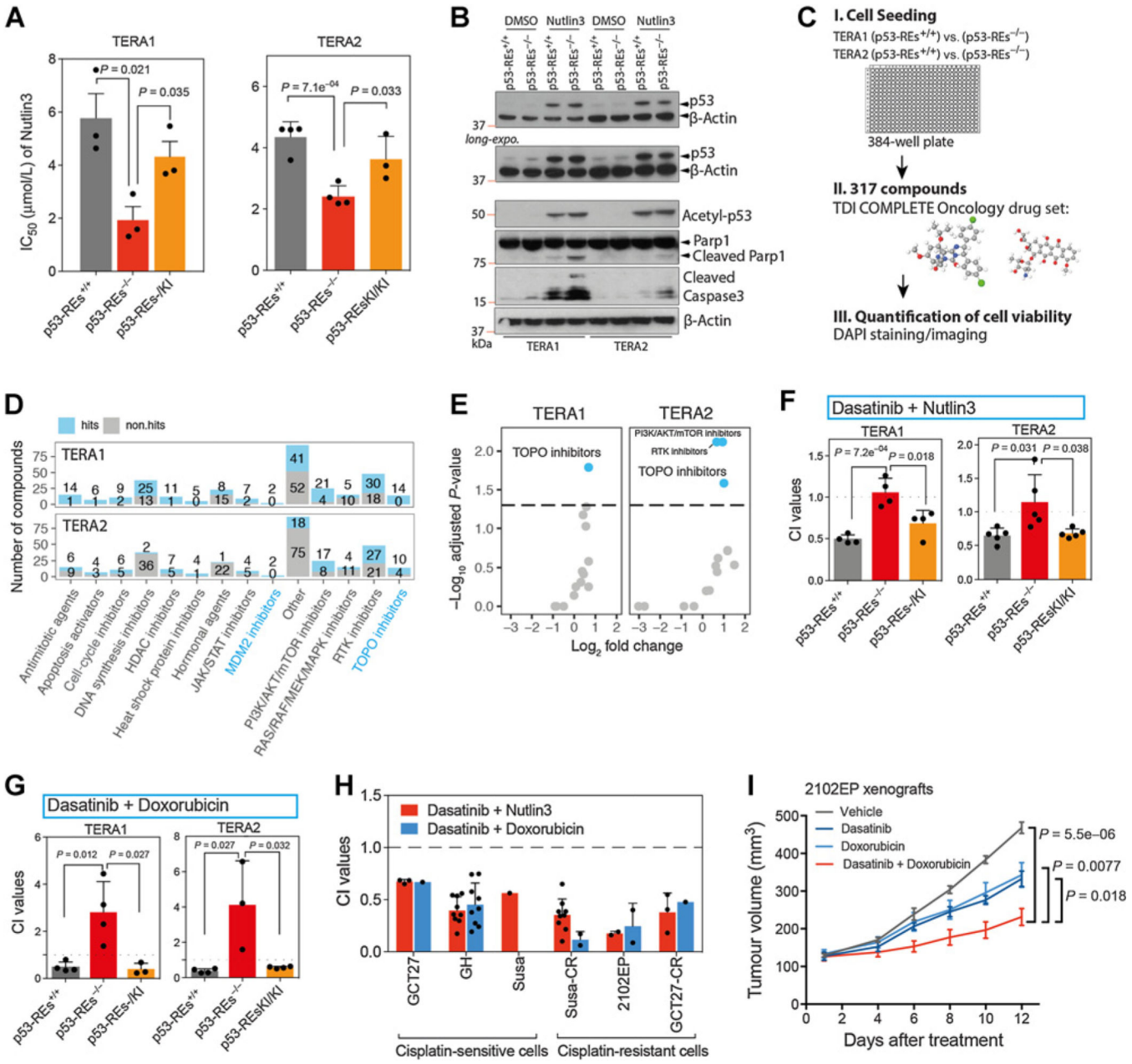

Figure 5.

p53/KITLG prosurvival signaling can attenuate responses to p53-activating agents. **A,** Bar blots of the IC_{50} values for Nutlin3. *P* values were calculated using a two-tailed *t* test and error bars represent SEM in at least three independent biological replicates. **B,** Western blot analysis of cells that were treated with or without Nutlin3 for 6 hours, lysed and analyzed for p53, acetylated p53, Parp1, and cleaved caspase-3 protein expression. **C,** Schematic overview for the microscopy-based high-content drug screening. **D,** Bar plots depicting the number of hits and "non-hits" for each of the 14 drug classes examined. **E,** Scatter plots of the fold enrichment of hits among each drug class relative to the total compounds in the 14 drug classes. The horizontal dashed lines represent the FDR-adjusted *P* value of 0.05. **F**

and **G,** Bar plots of combination indexes of dasatinib with Nutlin3 (**F**) or doxorubicin (**G**) in p53-REs$^{+/+}$ (gray bars, two clones), p53-REs$^{-/-}$ (red bars, two clones), and KI clones (orange bars, one clone) of TERA1 and TERA2 cells. **H,** Bar plots of combination indexes of dasatinib with Nutllin3 or doxorubicin in panel of TGCT cell lines. **I,** Growth curves of 2102EP xenograft tumors treated with vehicle, doxorubicin, dasatinib, or the combination of doxorubicin and dasatinib. Error bars, means ± SEM (n = 6).

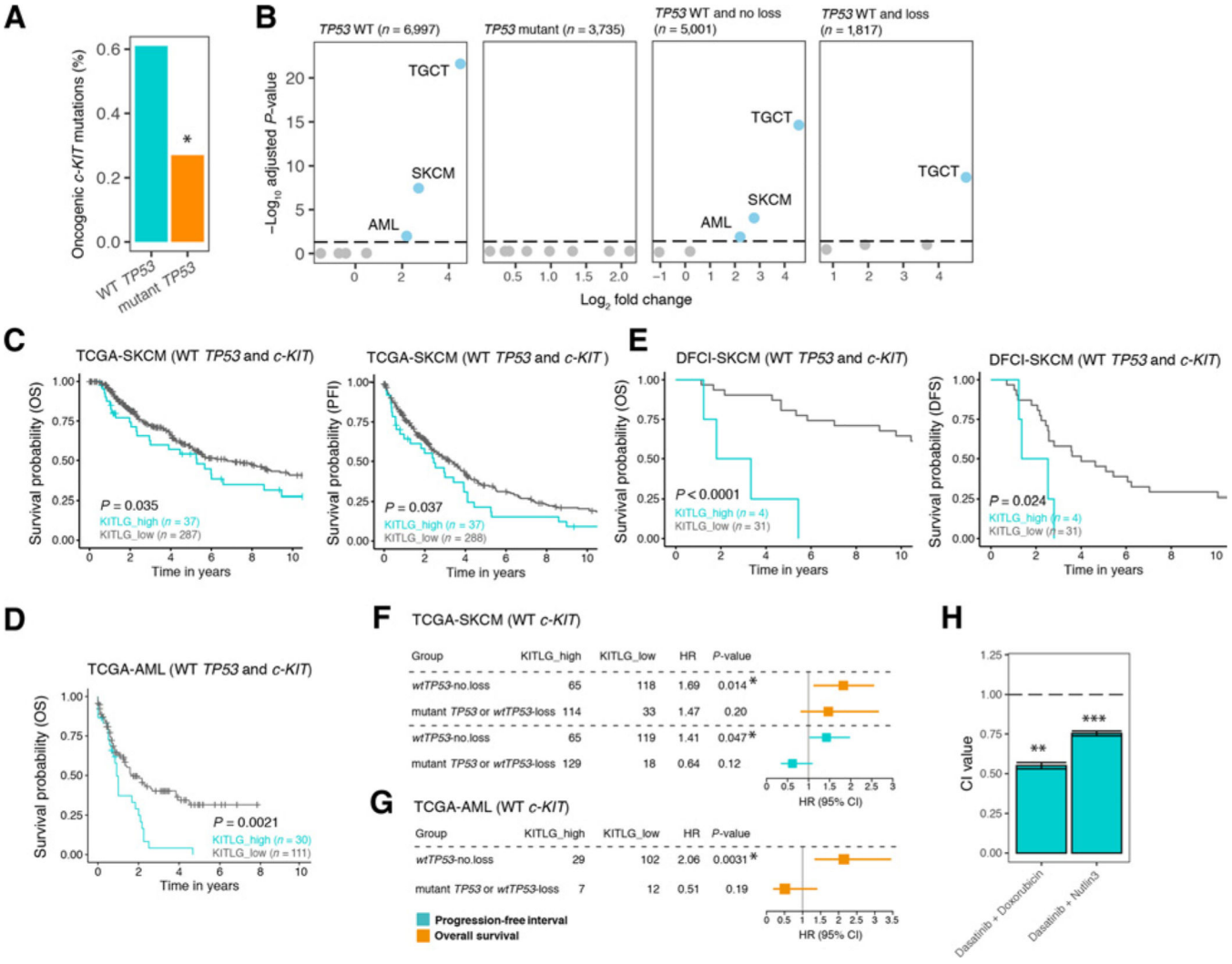

Figure 6.

KITLG/c-KIT signaling interacts with p53 to affect cancer progression and drug response in melanoma. **A,** A bar graph of the percentage of oncogenic *c-KIT* mutations in *wtTP53* tumors relative to *TP53* mutant tumors. *, $P = 0.014$. **B,** Scatter plots of the fold enrichment of oncogenic *c-KIT* mutations in a given cancer type relative to all cKIT mutations in pan-cancer. The horizontal dashed lines represent the FDR-adjusted *P* value of 0.05. **C–E,** Kaplan-Meier survival curves for OS (**C,** left) and PFI (**C,** right) in patients with TCGA–SKCM, for OS (**D**) in patients with TCGA–AML, and for OS (**E,** left) and DFS (**E,** right) in patients with DFCI–SKCM stratified on the basis of *KITLG* mRNA levels. **F** and **G,** Two forest plots of PFI and OS of TCGA cancer patients (**F,** SKCM; **G,** AML) stratified by the somatic *TP53* mutational status. HR and *P* values were calculated using Cox proportional hazards model. **H,** A bar plot of combination indexes of dasatinib with Nutlin3 or doxorubicin in melanoma cells. *P* values were calculated by one-sample *t* test. Error bars, means ± SEM ($n = 3$). **, $P = 0.00066$; ***, $P = 0.0013$.